DIFFUSE X-RAY SCATTER FROM MYOSIN HEADS IN ORIENTED SYNTHETIC FILAMENTS

F. R. POULSEN, J. LOWY, P. H. COOKE, E. M. BARTELS, G. F. ELLIOTT, AND R. A. HUGHES
Open University, Oxford Research Unit, Oxford OX1 5HR, United Kingdom

ABSTRACT X-ray results are presented concerning the structural state of myosin heads of synthetic filaments in threads. These were made from purified rabbit skeletal muscle myosin and studied by x-ray diffraction and electron microscopy by Cooke et al. (Cooke, P. H., E. M. Bartels, G. F. Elliott, and R. A. Hughes, 1987, *Biophys. J.*, 51:947–957). X-ray patterns show a meridional peak at a spacing of 14.4 nm. We concentrate here on the only other feature of the axial pattern: this is a central region of diffuse scatter, which we find to be similar to that obtained from myosin heads in solution (Mendelson, R. A., K. M. Kretzschmar, 1980, *Biochemistry*, 19:4103–4108). This means that the myosin heads have very large random displacements in all directions from their average positions, and that they are practically randomly oriented. The myosin heads do not contribute to the 14.4-nm peak, which must come entirely from the backbone. Comparison with x-ray data from the unstriated *Taenia coli* muscle of the guinea pig indicates that in this muscle at least 75% of the diffuse scatter comes from disordered myosin heads. The results confirm that the diffuse scatter in x-ray patterns from specimens that contain myosin filaments can yield information about the structural behavior of the myosin heads.

INTRODUCTION

In muscle research the so-called crossbridges have been studied intensively since they were first seen to project from the surface of thick filaments in electron micrographs of vertebrate skeletal muscle (Huxley, 1957). A crossbridge is composed of two subfragment-1 (S-1) heads and at least part of the subfragment-2 (S-2) rod portion of the myosin molecule (Lowey, 1979). The remaining portion of the myosin molecule, the light meromyosin, is assembled into a well-ordered filament backbone (Lowey, 1979). Nevertheless, x-ray experiments show that in living muscle the heads can have large random displacements that produce diffuse scatter, which contains information about the movement and orientation of the heads (Poulsen and Lowy, 1983). Because other muscle proteins, especially those that are soluble, could also scatter, it is important to confirm our results using a system composed only of myosin.

It is well known that at ionic strength ~0.6 myosin filaments of skeletal muscle dissolve, and that the molecules re-assemble into synthetic filaments as the ionic strength is lowered to ~0.2 (Huxley, 1963). In connection with investigations of the molecular charge on the myosin molecule (Bartels et al., 1985), threads of purified skeletal myosin have recently been prepared in our laboratory (Cooke et al., 1984). These threads are composed of oriented synthetic myosin filaments, as evidenced by the presence of a 14.4-nm meridional peak in x-ray patterns (Cooke et al., 1984).

In this paper we analyze the diffuse scatter in x-ray patterns from the myosin threads in terms of myosin head disorder, and compare its intensity level with that from living intact muscle. For this purpose the unstriated *Taenia coli* muscle of the guinea pig (TCGP) is a suitable muscle type, because here the order of the myosin filaments is similar to that in the myosin threads. In the TCGP muscle the only in vivo sign of myosin in filament form is the presence of a meridional peak with a spacing of 14.3 nm (Lowy et al., 1970).

METHODS

Preparation

The myosin threads were made from column-purified rabbit skeletal myosin using the procedures given by Cooke et al. (1987). The threads were checked for purity by SDS gel electrophoresis and no significant quantity of protein other than myosin was found. In the experiments the threads were maintained in a solution of 20 mM KCl, 1 mM $MgCl_2$, and 4 mM phosphate buffer at room temperature and pH 7.0. The ionic strength (0.03) is well below the threshold of ~0.2, which strongly favors filaments rather than dissolved molecules. Furthermore, before use the threads were washed for several hours in the 0.03 ionic strength solution to remove any free myosin molecules. We can therefore be certain that practically all the myosin molecules in the threads are included in the filaments. The electron micrographs described by Cooke et al. (1987) show that the myosin filaments in the threads vary somewhat in diameter and length, pack sideways with interfilament distances similar to those found in rabbit skeletal muscle A-band, and have a solid backbone surrounded by a continuous halo of lower density, which is most likely due to disordered crossbridges.

TCGP muscles were prepared as described by Lowy et al. (1970). The experiments described here were performed more recently (Lowy, J., and F. R. Poulsen, unpublished results). The muscles were kept at constant length, and their tension was monitored by a force transducer. They were

maintained in a normal mammalian Ringer solution perfused with a mixture of 95% O_2 and 5% CO_2. All the muscles used behaved normally in that they showed the usual spontaneous, rhythmic activity at 37°C. Experiments were carried out at temperatures ranging from 5° to 37°C. The spontaneous activity was reversibly abolished at temperatures below ~15°C.

RESULTS

X-Ray Diffraction

Using the synchrotron facility at Daresbury, Cooke et al. (1984, 1987) recorded x-ray patterns from the threads. One of these patterns, described in detail in the accompanying paper by Cooke et al. (1987), is shown in Fig. 1. A meridional reflection at 14.4 nm is clearly seen, but no off-meridional layer lines of the type seen in resting skeletal muscle (Elliott, 1964; Huxley and Brown, 1967) are visible. Instead, the patterns show a central region of strong diffuse scatter similar to that reported from intact muscles (Poulsen and Lowy, 1983) and from S-1 in solution (Mendelson and Kretzschmar, 1980).

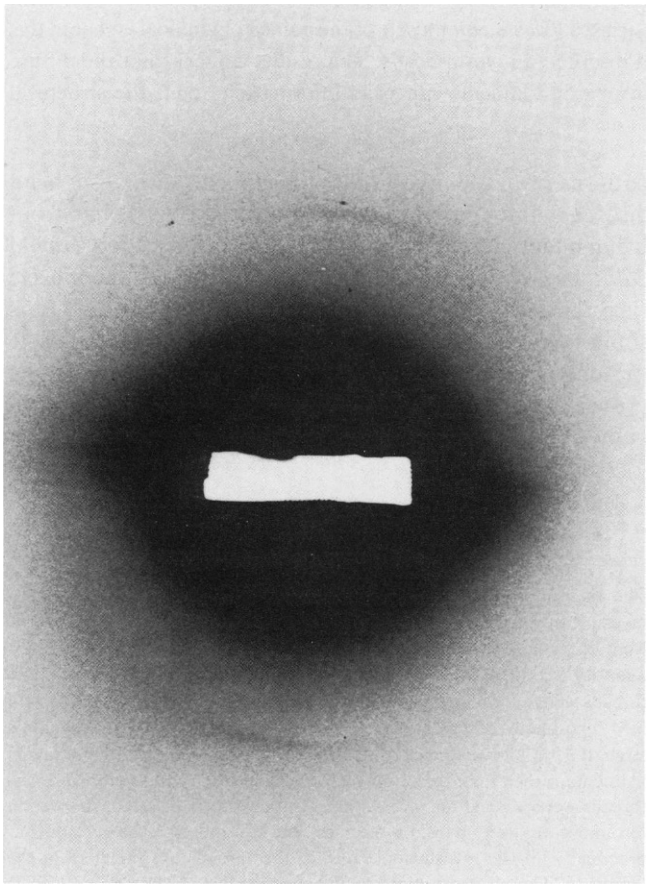

FIGURE 1 X-ray diffraction pattern from a myosin thread taken at the synchrotron radiation facility at Daresbury. The pattern was recorded on film using a low-angle scattering camera with a specimen-to-film distance of 2.2 m and an exposure time of ~30 min. The thread was mounted vertically in a cell equipped with mylar windows for the passage of x-rays. The meridional direction in the pattern is shown vertically. The main feature is a continuous region of slowly varying diffuse scatter. Note the presence of a meridional peak at spacing 14.4 nm and the absence of off-meridional myosin layer lines.

The TCGP muscle x-ray patterns were recorded on a 360-mm two-crystal camera using a GX13 Elliott Automation (Borehamwood, UK) rotating anode x-ray generator as the source. We found that lowering the temperature from 37°C to below ~15°C caused the 14.3-nm meridional peak to increase in intensity and to narrow in the lateral direction. We have analyzed patterns obtained at 8°C because at that temperature one obtains a peak sufficiently clear for our purpose (Fig. 3).

It was not necessary to correct for the instrumental background from either of the cameras since recordings without samples showed that it was insignificant compared with the sample scatter in the region of the patterns used. In both cameras the focal spots were much smaller than the 14.4-nm meridional peak both in the axial and the lateral direction. This means that the true peak dimensions in the patterns of both the threads and the TCGP were recorded. Because of the focusing of the beam in two dimensions, the sizes of the preparations are not important for the widths of the observed peaks. Thus no correction for instrumental parameters is necessary for comparing the 14.4-nm meridional peaks in the two preparations.

Densitometry

Tracings of the intensity distribution in the x-ray patterns were obtained by scanning the films in the axial direction with a Joyce–Loebl microdensitometer MK III C. The slit dimensions used in the axial and lateral directions were, respectively, 2.7×10^{-4} nm^{-1} and 2.9×10^{-3} nm^{-1} for the myosin threads (Fig. 2), and 1.8×10^{-3} nm^{-1} and 7.7×10^{-3} nm^{-1} for the TCGP muscles (Fig. 3). These slit dimensions are much smaller than the peaks in the patterns, so no correction for slit size is needed. The two-dimensional intensity distribution of the diffuse scatter from the myosin threads was composed from scans at ten different lateral positions (Fig. 4). For scaling purposes the integrated intensity of the 14.4-nm meridional peak was measured as follows. The patterns were scanned in the axial direction at five different lateral positions out to a distance of 0.035 nm^{-1} from the meridian where the peak was no longer visible. After background subtraction the peak intensity was integrated in the axial direction, thus producing the intensity profile in the lateral direction. The volume defined by a full rotation of this profile about the intensity axis was then taken to be the integrated intensity of the 14.4-nm peak.

DISCUSSION

Structural Implications

Since myosin is the only protein present in the thread preparation, both the 14.4-nm meridional peak and the diffuse scatter must come from myosin molecules. That

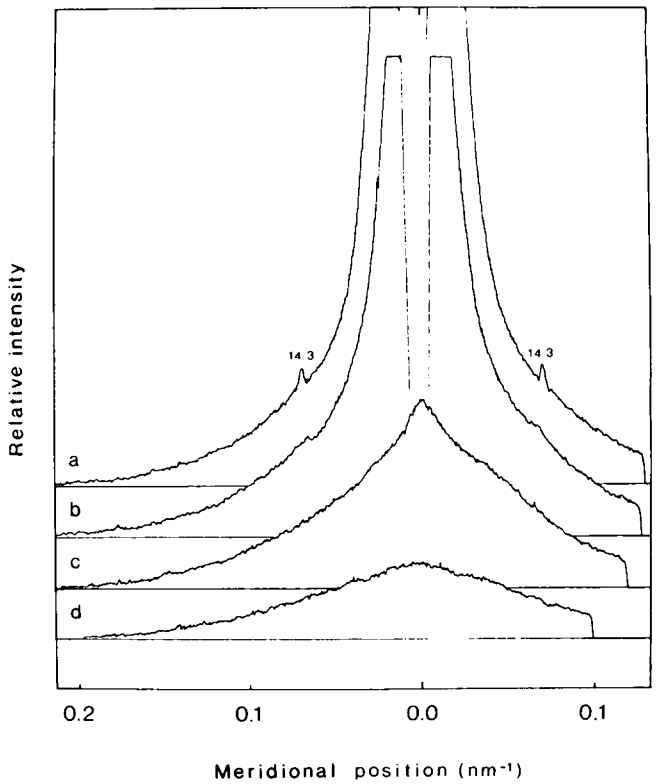

FIGURE 2 Densitometer tracings of the intensity distribution in the pattern shown in Fig. 1. Tracings *a–d* are, respectively, along the meridian and parallel to it at lateral distances 0.0234, 0.0586, and 0.0937 nm^{-1}. The diffuse scatter dominates the pattern rising steeply towards the center. The meridional tracing shows the 14.4-nm peak, so characteristic of myosin filaments. Its axial width is only 2.7×10^{-3} nm^{-1} (FWHM), demonstrating that the filaments are well-ordered in the axial direction. The other tracings demonstrate the absence of any off-meridional myosin layer lines of the type seen in resting vertebrate striated muscle. Also, there are no signs that the intensity of the diffuse scatter between the equator and the 14.4-nm peak decreases towards zero, as would be expected if the myosin head arrangement had any significant axial order.

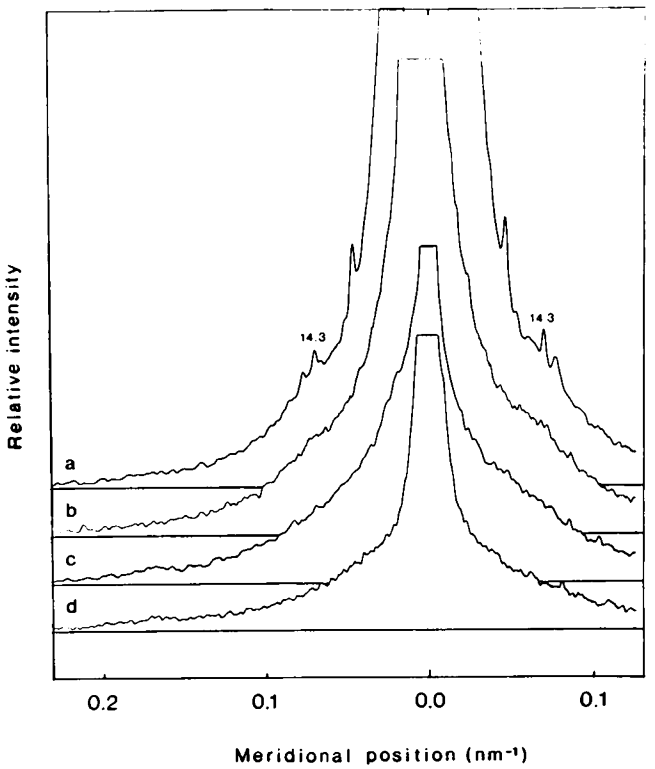

FIGURE 3 Tracings of the intensity distribution in an x-ray diffraction pattern from a TCGP muscle maintained in normal Ringer at 8°C. The pattern was taken on a 360-mm two-crystal camera using an Elliott Automation GX13 rotating anode x-ray generator. The exposure time was 42 h. Tracings *a–d* are, respectively, along the meridian and parallel to it at lateral distances 0.0309, 0.0618, 0.0927 nm^{-1}. The diffuse scatter dominates the pattern rising steeply towards the center. The meridional tracing (*a*) shows the 14.3-nm peak from the myosin filaments with an axial width of 3.07×10^{-3} nm^{-1}, as well as peaks from collagen filaments at spacings 21.7 and 13.0 nm. The other tracings demonstrate that the pattern is similar to the myosin thread pattern in that it lacks off-meridional layer lines of the type seen in resting striated muscle and any other signs of myosin head order in terms of fast modulations of the diffuse scatter.

these two features of the pattern show such a large difference in axial width (Figs. 1 and 2) means that they originate from two parts of the molecule with very different degrees of order. The very narrow 14.4-nm peak can only be due to a part assembled in the meridional direction with long-range order over many molecules, whereas the diffuse scatter (which is ~50 times broader) must come from a part that is so disordered that one sees its molecular transform. Because the backbone is a continuous structure from which the myosin heads project, the only realistic assignment is that the backbone constitutes the well-ordered component, whereas the myosin heads have total disorder. This interpretation is consistent with our finding (illustrated in Fig. 4) that the intensity distribution of the diffuse scatter from the threads is very similar to that obtained by Mendelson and Kretzschmar (1980) from myosin heads in solution.

A measure for the axial extent of the order in the backbone can be obtained from the axial width of the 14.4-nm peak. For this purpose we use the formula

$$I(\Delta Z) = [\sin(N\pi\Delta Z a)/\sin(\pi\Delta Z a)]^2 \qquad (1)$$

for the axial profile of the peak, where N is the number of coherently diffracting units, a is their axial repeat distance, and ΔZ is the distance in reciprocal space from the peak maximum. The full width at half maximum (FWHM) of the 14.4-nm peak is 2.7×10^{-3} nm^{-1} (Fig. 2). With a = 14.4 nm we find that N becomes 23. This means that the axial long-range order of the filament backbone is maintained for at least 23 × 14.4 nm = 331 nm.

At this stage it is necessary to consider what types of disorder can exist in the backbone and in the arrangement of the myosin heads. Because the heads are attached to the backbone through a flexible link, they are free to move about and will undergo Brownian motion. However, on average they will take up an ordered arrangement determined by the structure of the backbone. This is because the

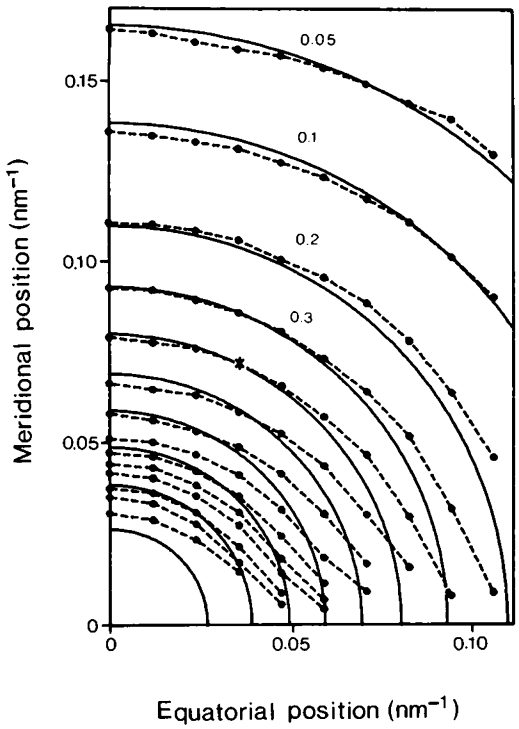

FIGURE 4 Contour maps comparing the scattered intensity in patterns from synthetic myosin filaments (-●-) and from S-1 in solution (—) using for the latter the data published by Mendelson and Kretzschmar (1980). The synthetic filament data come from the experiments described in Fig. 2. To obtain the level curves three patterns were scanned in the meridional direction at 10 different lateral positions and averaged over the symmetry-related parts. The S-1 solution curves were reconstructed by Fourier inversion of the distance distribution function published as Fig. 3 in Mendelson and Kretzschmar (1980). The intensity levels are 0.05, 0.10, 0.20, 0.30, 0.40, 0.50, 0.60, 0.70, 0.80, 0.90, 1.00, 1.25, 1.50, and 2.00; the last three only for the thread data. The intensity values of the two data sets were scaled together at (*). There is an excellent agreement between the two data sets over the major part of the pattern. The thread diagram has very nearly circular symmetry with a small compression in the axial direction. Two specific regions show deviations. Toward the center in the meridional direction the thread intensity is somewhat below, whereas even further in toward the center it catches up with and then exceeds that of the solution data. In the threads this type of deviation is expected from an interference between the two heads of the myosin molecule if the heads are on average located axially above each other. Note that the circular symmetry in the thread diagram is also perturbed due to some extra intensity spreading out from the equator. This is to be expected due to contributions from the filament backbone and the S-2 rods.

force restoring a head toward the position determined by the backbone increases with the displacement. The functioning of the backbone as a reference structure for the myosin heads also means that the loss of order between two heads due to their movement does not accumulate with increasing distance between them (type-1 disorder). Thus the long-range order of the heads is maintained to the extent that it is present in the backbone. Being a relatively rigid structure, the backbone will have much less disorder than the myosin heads, but that disorder will be of a different type. This is because the backbone does not have a reference structure that can be the basis for a restoring force, and therefore any disorder that occurs from one molecule to the next will accumulate with increasing distance between two molecules (type-2 disorder). It follows that in principle the long-range order can break down in the backbone, but in practice will do so only to a small extent. The root mean square displacement between neighboring molecules Δ_2 is only 0.89 nm (see Appendix).

The two types of disorder have two very different effects on the intensity of the peaks in the x-ray pattern: type-1 disorder does not affect the width of a peak, but reduces its overall intensity by the Debye–Waller factor (D) that decreases exponentially with the square of the root mean square (rms) displacement (Δ_1) of the molecules and the square of the distance (s) in reciprocal space from the center of the pattern:

$$D = \exp(-4\pi^2\Delta_1^2 s^2/3) \quad (2)$$

Type-2 disorder causes the width of a peak to increase, but this is compensated by a decrease in height, so the integrated intensity remains constant. This can be seen from the three formulae given by Vainshtein (1966):

$$I_{max} = 1/(\pi^2 h^2(\Delta_2/a)^2) \quad (3)$$

$$W = (1/a)\pi^2 h^2(\Delta_2/a)^2 \quad (4)$$

$$A = I_{max}W = 1/a. \quad (5)$$

I_{max} is the height of the peak, W is its integral half-width (ratio of its area to its height), h is the order of the peak, Δ_2 is the rms displacement between first neighbors of molecules, a is the mean distance between nearest neighbors, and A is the area or integral over the peak. These formulae hold accurately when $h\Delta^2/a$ is smaller than ~0.2.

Practically all the myosin heads in the threads must have large random displacements from their average positions in all directions. If for example a significant fraction of them were displaced only in the radial and azimuthal but not in the axial direction (thus on average forming discs of high electron density with an axial repeat of 14.4 nm), they could not produce scatter free of ripples in the meridional direction. Rather, their scatter would be sampled into layer lines with a 14.4-nm axial repeat. The intensity between these layer lines from the axially ordered heads would be very low, but the scatter shows no modulations of this kind (Fig. 2).

As described above, the myosin heads are subject to type-1 (thermal) disorder. In that case the intensity of the diffuse scatter is zero in the center of the pattern (Guinier, 1963; Vainshtein, 1966). That the heads nevertheless produce scatter at low angles in x-ray patterns from muscle was explained in terms of type-1 disorder with a very large rms displacement (Δ_1) (Poulsen and Lowy, 1983). Consequently the intensity rises from zero in the center of the pattern to a maximum whose distance (s) from the center decreases as (Δ_1) increases. In frog skeletal muscle

(Poulsen and Lowy, 1983) we were able to follow the scatter in to a distance $s_{min} = 0.04$ nm^{-1} and observed no visible intensity drop, which indicates that Δ_1 is at least 9 nm. For the thread pattern s_{min} is 0.01 nm^{-1}, which corresponds to Δ_1 being at least 50 nm. That the latter value exceeds the 43-nm axial unit cell length confirms that the heads are totally disordered, also axially. This is consistent with the absence of any off-meridional layer lines of the type seen in resting skeletal muscle and which index on a 43-nm repeat. It also follows that in the threads the myosin heads do not contribute to the 14.4-nm meridional peak, which must therefore come entirely from the filament backbone. With $\Delta_1 = 50$ nm and $s = 1/14.4$ nm, Eq. 2 shows that the Debye–Waller factor reduces the intensity to zero while, as explained above, there will be no reduction in the contribution from the backbone with type-2 disorder to the integrated intensity of the 14.4-nm peak.

The same situation applies to the TCGP muscle. The diffuse scatter shows no signs of a decrease in intensity between the equator and the 14.3-nm layer line (Fig. 3), which means that in the TCGP the myosin heads have large random displacements in all directions. As expected from this conclusion, no off-meridional layer lines are seen.

In resting frog skeletal muscle Poulsen and Lowy (1983) found that about half of the myosin heads takes part in an ordered array, which is responsible for the layer lines. The other half was found to be disordered, producing diffuse scatter and not contributing to the layer lines. Is it possible that a similar situation exists in the myosin threads and in the TCGP, and in that case one wonders if a small fraction of ordered heads could contribute to the 14.4-nm meridional peak but produce layer lines so weak, they would be masked by the strong superimposed background. We do not consider this to be likely because in the frog muscle one of the strongest parts of the myosin pattern is the first layer line of spacing 42.9 nm, which should therefore be visible in the thread and TCGP patterns if a significant fraction of myosin heads was ordered. In resting frog skeletal muscle some of the weaker parts of the myosin layer lines are superimposed on a background that is more than 20 times as strong. Yet these layer lines are clearly visible (unless the pattern is overexposed). There can therefore be no doubt that if there existed a population of ordered myosin heads large enough to contribute to the 14.4-nm meridional peak, then such heads would also produce a visible layer line at 42.9 nm.

The main part of the scattering pattern from the threads has nearly circular symmetry (Fig. 4). A small compression in the axial direction indicates that the heads have a slight preferential orientation with their long axis in that direction. Comparison of the thread pattern with that from S-1 in solution (Mendelson and Kretzschmar, 1980) shows that close to the center the intensity of the thread scatter is higher (Figs. 4 and 5). This is to be expected as in the thread there will be interference between the two heads of the myosin molecule. Close to the meridian, between the higher central intensity and the outer part of the pattern, there is a region of intensity lower than that seen in the solution scatter (Fig. 4). This indicates that on average the two heads are located axially above each other. Because over most of the pattern there is excellent agreement between the thread and solution scatter (Fig. 5), the contribution from the S-2 rods must be negligible except close to the equator. There we find indeed that the intensity is higher (Fig. 4) than could be given by the heads alone. This is what one would expect because, due to spatial restrictions, the long thin rods (40-nm long, 2-nm diam; Lowey, 1979) will have a strongly preferred orientation and make a rather small angle relative to the direction of the fiber axis. Thus any scatter produced by the rods will be concentrated near the equator. An object with the dimensions of the rods will give a scattering curve whose intensity has diminished to zero at a distance of 0.025 nm^{-1} from the center of the pattern in the direction of the long axis.

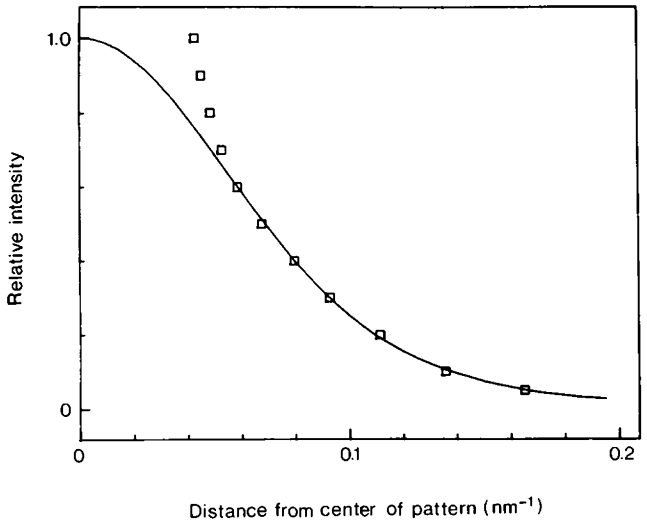

FIGURE 5 Comparison of intensity profiles taken in a direction of 30° from the meridian where the modulations due to head interference and equatorial diffraction have the smallest effect. Data for S-1 in solution (—) come from Mendelson and Kretzschmar (1980); those for the myosin thread (□) from Fig. 3. Note the excellent agreement outside a distance of 0.05 nm^{-1} from the center of the pattern. The larger intensity of the thread data closer to the center is due to the interference between the two heads of the myosin molecule.

Comparison with TCGP Muscle Data

Inspection of the meridional tracings in Figs. 2 *a* and 3 *a* suggests that the intensity of the scatter is slightly greater in the TCGP muscle. For a rigorous comparison the two data sets should be brought to the same scale. The only feature of the myosin thread pattern suitable for this purpose is the 14.4-nm meridional peak. Before accepting that this peak can be used as a standard, we will consider

the possible factors that can influence its intensity relative to that of the scatter from the myosin heads.

In preparations like the myosin threads and the TCGP muscle where the myosin heads have large random displacements there is no definite phase relationship between x-rays scattered from them. Hence the total intensity is directly proportional to the number of heads, rather than to the square of their number. In the Appendix we demonstrate that also the intensity of the 14.4-nm peak integrated both in the axial and the lateral directions is directly proportional to the number of molecules present in filament form. The integrated intensity of the 14.4-nm peak can thus be used as a reference parameter for the comparison of the diffuse scatter from myosin threads and TCGP muscles.

The intensities of the 14.4-nm peaks in the TCGP muscle and the myosin thread were measured and integrated as described above and their ratio multiplied with the level of scatter measured near the 14.4-nm peak on the thread pattern to give the expected level of scatter in the TCGP. Comparison with the observed level indicates that ~75% of the TCGP muscle scatter comes from disordered myosin heads organized into filaments.

Here it is relevant to mention the well-known difference in the solubility between myosin from striated and smooth vertebrate muscle. Whereas myosin from striated muscle dissolves only at a relatively high ionic strength (0.6 M KCl is normally used), Laszt and Hamoir (1961) found that smooth muscle myosin is soluble at a much lower ionic strength (0.06 M KCl) in the presence of 1 mM ATP. Smooth muscle myosin extracted at low ionic strength also forms synthetic filaments with well-ordered backbones and visible projections (Sobieszek, 1972). In smooth muscle the balance between myosin filaments and molecules in solution depends on several factors several factors such as light chain phosphorylation (Suzuki et al., 1978) and the concentration of ATP, Mg^{2+}, and Ca^{2+} (Shoenberg and Stuart, 1980).

Our x-ray data cannot exclude the possibility that some of the myosin molecules are in solution in the living TCGP muscle. Clearly, the dissolved myosin molecules will contribute to the diffuse scatter, but not to the 14.3-nm peak. Thus some of the remaining 25% of the scatter from the TCGP muscle may also be due to myosin heads. The overall conclusion is that at least 75% of the diffuse scatter seen in the TCGP muscle comes from disordered myosin heads. The remaining scatter might come from soluble proteins.

RELATION TO OTHER WORK

Our conclusion that in the thread preparation the myosin heads are totally disordered with respect to both the location of their mass centers and their orientation is in line with several other observations. In non-overlap rigor skeletal muscle the myosin filaments exist under conditions similar to those in the threads (i.e., absence of ATP and actin filaments). Therefore the arrangement of myosin heads in the two systems might also be expected to be similar. Indeed, total disorder in the location of the myosin heads in non-overlap, rigorized frog skeletal muscles has been established by x-ray experiments (Haselgrove, 1975*a*; Poulsen and Lowy, 1983). The x-ray data of Poulsen and Lowy (1983) also suggested that the heads in the non-overlap rigor muscle are practically randomly oriented. Similar results have been found in electron paramagnetic resonance (EPR) studies of spin-labeled myosin heads. Using the EPR technique on glycerinated rabbit psoas fibers Thomas and Cooke (1980) found that at full overlap between actin and myosin filaments and in the absence of ATP, the myosin heads are highly oriented, whereas at non-overlap or in the presence of ATP, they are highly disoriented. Data from saturation transfer EPR studies of spin-labeled rabbit psoas muscle fibers in the absence of ATP (Barnett and Thomas, 1984) support the above conclusions. Thus myosin heads in the overlap zone were found to be immobilized, whereas those in the non-overlap zone have very high rotational mobility.

The result that at least 75% of the diffuse scatter seen in the TCGP muscle comes from disordered myosin heads agrees with SDS PAGE studies of the soluble proteins extracted from fresh TCGP muscles by Tregear and Squire (1973). Inspection of their plate I, column 5, clearly shows that bands containing soluble proteins with molecular weights comparable to myosin are dominated by myosin and actin. In intact muscles actin is organized into filaments that produce layer lines in the x-ray pattern, and therefore no scatter. Large amounts of soluble very low molecular weight proteins that do not show up on the gel may of course be present. But such proteins would only contribute a very flat scattering profile to the x-ray pattern. According to Tregear and Squire (1973) the insoluble residue consists principally of collagen. Again in intact muscles the collagen is organized into filaments that produce narrow peaks on the meridian of the x-ray pattern (see Fig. 3 *a*) and therefore no diffuse scatter.

Our finding that at least 75% of the scatter from the TCGP muscle is due to myosin heads is also in agreement with the estimate of 85%, which we obtained for frog skeletal muscle (Poulsen and Lowy, 1983). There is of course no reason why the two values should be exactly the same, considering the difference in the biochemical composition of these two muscle types.

Our data from living muscle and myosin threads suggest that the main part of the myosin head mass is contained within a length of ~12 nm as determined for S-1 by x-ray solution scattering (Mendelson and Kretzschmar, 1980). In contrast, under various conditions, the length of the myosin head has been found to range from 10 to 20 nm (based on electron microscope determinations by Elliott and Offer, 1978; Takahashi, 1978; Amos et al., 1982; Vibert and Craig, 1982; Knight and Trinick, 1984), and a

contour length of 16 nm was deduced from a study of S-1 crystals (Winkelmann et al., 1985). This suggests that the shape of the heads may not be the same in these various preparations. Such an idea receives support from the recent discovery (Craig et al., 1985) that in the presence of ATP, myosin heads bound to actin are shorter and fatter than in the absence of ATP. It should however also be noted that a relatively thin region of the myosin head which might extend a few nanometers from the main mass would not contribute much to the x-ray scattering pattern but could very likely attract enough stain to be seen in the electron microscopy data.

CONCLUSIONS

The results presented here lead to the conclusion that although the filament backbone is well-ordered, the myosin heads in the threads of synthetic myosin filaments are totally disordered as far as the location of their mass centers is concerned. They also have a wide range of orientations with a slight preference towards the axial direction.

Furthermore, our results show that at least 75% of the diffuse scatter in x-ray patterns from intact TCGP muscles comes from disordered myosin heads. Together with our previous result that ~85% of the diffuse scatter present in x-ray patterns from living frog skeletal muscles comes from myosin heads (Poulsen and Lowy, 1983), our present observations mean that there is now a very strong case for using the diffuse scatter to study the structural behavior of heads in contracting muscles. This will supplement the information that can be extracted from the myosin layer lines where certain factors make it difficult to interpret the data. The layer lines are due to the regularity in the average arrangement of crossbridges (Elliott, 1964; Huxley and Brown, 1967). In this case, the phase relationship between the x-rays scattered from myosin heads in different parts of the structure is very important. The diffraction pattern is therefore very sensitive to changes in the order of crossbridges, both within and between filaments. Moreover, the presence of statistical disorder in the orientation of the thick filaments in all striated muscles studied so far except the bony fish muscle (Harford and Squire, 1986) adds to these difficulties. In contrast, the diffuse scatter is produced by myosin heads which, being totally disordered, scatter the x-rays independently. Therefore any change in the level or distribution of scattered intensity reflects directly a change in number, shape, or orientation of disordered myosin heads.

Regarding the ordered arrangement, experiments with living muscles do indeed demonstrate that this breaks down during contraction and that many of the features of the myosin layer line system disappear while no signs of any other kind of order can be detected (Huxley and Brown, 1967; Elliott et al., 1967; Huxley et al., 1983). In contrast, recent studies of the diffuse scatter from contracting muscles show changes in its intensity distribution, which indicates that there is a definite relationship between the distribution of orientations of myosin heads and tension development and shortening of the muscle (Lowy and Poulsen, 1982, 1987).

APPENDIX

Effects of Various Structural Parameters on the Integrated Intensity of the 14.4-nm Meridional Peak

The Appendix explains why the integrated intensity of the 14.4-nm meridional peak is directly proportional to the number of myosin molecules present in filament form.

Our finding that the 14.4-nm peak comes entirely from the backbone simplifies matters considerably. If myosin heads had contributed to the 14.4-nm meridional peak the situation would have been more complicated, partly because there would be an unknown effect of interference between backbone and myosin heads, and partly because the heads are subject to type-1 disorder. This means that their contribution to the 14.4-nm peak could vary by a large factor with no compensation in the width of the peak.

As explained above, because the backbone can have type-2 disorder only, and provided $h\Delta_2/a$ is relatively small, any loss in peak height due to an increase in disorder is compensated for by a widening of the peak so that the integrated intensity remains constant. With $a = 14.4$ nm, $W = 2.7\ 10^{-3}$ nm^{-1}, and $h = 1$, Eq. 4 gives $\Delta_2 = 0.89$ nm. Thus $h\Delta_2/a$ is 0.062, which is small enough for Eqs. 3–5 to apply.

In the filament backbone the axial displacement between successive levels of myosin molecules is obviously 14.4 nm in both the myosin threads and the muscle. Therefore the variation in electron density along the filament axis is the same in the two preparations, and so is the form factor contributing to the intensity from each unit cell.

What about differences in length of the filaments? In his treatment of type-2 disorder, Vainshtein (1966) does not explicitly give the dependence of the peak height on the length of the filament. However, as long as $h\Delta_2/a$ is relatively small, as it is here, the area under the peak is the same as that of the zero-order one. The latter does not depend on the disorder. Its height is simply proportional to the square of the number of molecules (or filament length), and its axial width is inversely proportional to the filament length. Thus its intensity integrated in the axial direction is proportional to the filament length, and the same holds for the 14.4-nm peak. But the number of myosin heads is also proportional to filament length, and therefore the ratio of the intensity of the scatter to the intensity of the 14.4-nm meridional peak integrated in the axial direction is independent of filament length.

Differences in lateral dimensions can also be considered in light of the effect due to sideways aggregation of filaments. This is an important issue, because aggregation occurs in the TCGP muscle as evidenced by changes in the lateral profile of the 14.3-nm meridional peak due to changes in the experimental conditions. Thus, as mentioned above, cooling of the muscle from 37°C to below 15°C causes the 14.3-nm peak to become narrower in the lateral direction and at the same time to increase in height. This means that several filaments have aggregated to form a wider structure. Such structures have indeed been visualized in the electron microscope (Lowy and Small, 1970). Furthermore, Shoenberg and Haselgrove (1974) concluded from their observation of an increase in the intensity of the 14.3-nm peak that aggregation takes place on cooling (see also reviews by Haselgrove, 1975*b*; and Cooke, 1983). However, in the following we show that such aggregation does in fact not affect the integrated intensity of the 14.3-nm peak.

Let us consider what happens when two filaments combine sideways to form a larger unit. This will diffract coherently, so its peak intensity is proportional to the square of its mass. Because the mass of the larger unit

is up by a factor of two, its peak intensity will be four times that from each of the smaller units. But the number of units is halved, so the result is an increase in peak intensity by a factor of two. At the same time the width of the peak in the direction connecting the two units decreases by a factor of two. Therefore the total intensity of the two-dimensional peak in the lateral plane remains unchanged. Although the lateral profile of the peak from an individual unit now depends on the azimuthal direction, the random orientation of the filaments about the axial direction ensures that a cylindrically averaged profile is recorded on the film. No intensity is lost or gained in such an average. Therefore the total integrated intensity in two dimensions remains the same and can be calculated as the volume encircled by a full rotation about the intensity axis of the observed intensity profile.

One very important factor that affects the intensity of the 14.3-nm meridional peak in frog skeletal muscle is the variable sampling due to differences in the degree of three-dimensional order in the packing of the filaments into a hexagonal lattice (Huxley et al., 1982). Although that effect could be corrected for, this is not required for the myosin threads or the TCGP muscle, because here no three-dimensional interfilament order is present, as can be concluded from the absence of any sampling effects on the 14.3-nm layer line. Furthermore, both the electron microscopy evidence and the absence of any sharp peaks on the equator in x-ray patterns show that in their sideways packing the filaments lack even good two-dimensional order. The latter is of course a requirement for good three-dimensional order.

It appears that independent of various structural parameters, which might vary for the myosin filaments, the intensity of the 14.4-nm peak integrated both along the axial direction and in the lateral directions is directly proportional to the number of myosin molecules present in filament form.

We thank Mr. A. C. Elliott, Dr. C. Nave, Ms. R. S. Rapley, and Mr. P. E. Thomas for their assistance, and Dr. D. A. Blackburn and other members of the staff at the Oxford Research Unit for their support.

We are grateful for grants from the Medical Research Council (grant No. G8315930CB), Science and Engineering Research Council (grant Nos. GRC26521 and GRC77379), and the Muscular Dystrophy Association of America.

Received for publication 19 May 1986 and in final form 15 January 1987.

REFERENCES

Amos, L. A., H. E. Huxley, K. C. Holmes, R. S. Goody, and K. A. Taylor. 1982. Structural evidence that myosin heads may interact with two sites on F-actin. *Nature (Lond.).* 299:467–469.

Barnett, V. A., and D. D. Thomas. 1984. Saturation transfer electron paramagnetic resonance of spin-labeled muscle fibres. Dependence of myosin head rotational motion on sarcomere length. *J. Mol. Biol.* 179:83–102.

Bartels, E. M., P. H. Cooke, G. F. Elliott, and R. A. Hughes, 1985. Donnan potential changes in rabbit muscle A-bands are associated with myosin. *J. Physiol. (Lond.).* 358:80P.

Cooke, P. H. 1983. Organization of contractile fibers in smooth muscle. *Cell Muscle Motil.* 3:57–77.

Cooke, P. H., E. M. Bartels, G. F. Elliott, and K. Jennison. 1984. Myosin threads. *Biophys. J.* 45(2, Pt. 2):7a. (Abstr.)

Cooke, P. H., E. M. Bartels, G. F. Elliott, and R. A. Hughes. 1987. A structural study of gels, in the form of threads, of myosin and myosin rod. *Biophys. J.* 51:947–957.

Craig, R., L. E. Greene, and E. Eisenberg, 1985. Structure of the actin-myosin complex in the presence of ATP. *Proc. Natl. Acad. Sci. USA.* 82:3247–3251.

Elliott, A., and G. Offer. 1978. Shape and flexibility of the myosin molecule. *J. Mol. Biol.* 123:505–519.

Elliott, G. F. 1964. X-ray diffraction studies on striated and smooth muscles. *Proc. R. Soc. Ser. B.* 160:467–472.

Elliott, G. F., J. Lowy, and B. M. Millman. 1967. Low-angle X-ray diffraction studies of living striated muscle during contraction. *J. Mol. Biol.* 25:31–45.

Guinier, A. 1963. X-ray Diffraction in Crystals, Imperfect Crystals, and Amorphous Bodies. Freeman, Cooper & Co., San Francisco. 151–169, 185–209.

Harford, J., and J. Squire. 1986. "Crystalline" myosin cross-bridge array in relaxed bony fish muscle. Low-angle x-ray diffraction from plaice fin muscle and its interpretation. *Biophys. J.* 50:145–155.

Haselgrove, J. C. 1975*a*. X-ray evidence for conformational changes in the myosin filaments of vertebrate striated muscle. *J. Mol. Biol.* 92:113–143.

Haselgrove, J. C. 1975*b*. Structural changes in smooth and striated muscle during contraction. *In* Comparative Physiology. Functional Aspects of Structural Materials. Elsevier North-Holland Publishing Company, Amsterdam. 127–138.

Huxley, H. E. 1957. The double array of filaments in cross-striated muscle. *J. Biophys. Biochem. Cytol.* 3:631–648.

Huxley, H. E. 1963. Electron microscope studies on the structure of natural and synthetic protein filaments from striated muscle. *J. Mol. Biol.* 7:281–308.

Huxley, H. E., and W. Brown. 1967. The low-angle X-ray diagram of vertebrate striated muscle and its behaviour during contraction and rigor. *J. Mol. Biol.* 30:383–434.

Huxley, H. E., A. R. Faruqi, M. Kress, J. Bordas, and M. H. J. Koch. 1982. Time-resolved X-ray diffraction studies of the myosin layer-line reflections during muscle contraction. *J. Mol. Biol.* 158:637–684.

Huxley, H. E., R. M. Simmons, A. R. Faruqi, M. Kress, J. Bordas, and M. H. J. Koch. 1983. Changes in the X-ray reflections from contracting muscle during rapid mechanical transients and their structural implications. *J. Mol. Biol.* 169:469–506.

Knight, P., and J. Trinick. 1984. Structure of the myosin projections on native thick filaments from vertebrate skeletal muscle. *J. Mol. Biol.* 177:461–482.

Laszt, L., and G. Hamoir. 1961. Etude par electropherese et ultracentrifugation de la composition proteinique de la couche musculaire des carotides de bovide. *Biochem. Biophys. Acta.* 50:430–449.

Lowey, S. 1979. Fibrous Proteins: Scientific, Industrial and Medical Aspects. Academic Press, Inc., New York. 1–25.

Lowy, J., F. R. Poulsen, and P. J. Vibert. 1970. Myosin filaments in vertebrate smooth muscle. *Nature (Lond.).* 225:1053–1054.

Lowy, J., and J. V. Small. 1970. The organisation of myosin and actin in vertebrate smooth muscle. *Nature (Lond.).* 227:46–51.

Lowy, J., and F. R. Poulsen. 1982. Time-resolved X-ray diffraction studies of the structural behaviour of myosin heads in a living contracting unstriated muscle. *Nature (Lond.).* 299:308–312.

Lowy, J., and F. R. Poulsen. 1987. X-ray study of myosin heads in contracting frog skeletal muscle. *J. Mol. Biol.* In press.

Mendelson, R. A., and K. M. Kretzschmar. 1980. Structure of myosin subfragment 1 from low-angle X-ray scattering. *Biochemistry.* 19:4103–4108.

Poulsen, F. R., and J. Lowy. 1983. Small-angle X-ray scattering from myosin heads in relaxed and rigor frog skeletal muscles. *Nature (Lond.).* 303:146–152.

Shoenberg, C. F., and J. C. Haselgrove. 1974. Filaments and ribbons in vertebrate smooth muscle. *Nature (Lond.).* 249:152–154.

Shoenberg, C. F., and M. Stewart. 1980. Filament formation in smooth muscle. *J. Muscle Res. Cell Motil.* 1:117–126.

Sobieszek, A. 1972. Cross-bridges on self-assembled smooth muscle myosin filaments. *J. Mol. Biol.* 70:741–744.

Suzuki, H., H. Onishi, K. Takahashi, and S. Watanabe. 1978. Structure and function of chicken gizzard myosin. *J. Biochem.* 84:1529–1542.

Takahashi, K. 1978. Topography of the myosin molecule as visualized by an improved negative staining method. *J. Biochem.* 83:905–908.

Thomas, D. D., and R. Cooke, 1980. Orientation of spin-labeled myosin heads in glycerinated muscle fibres. *Biophys. J.* 32:891–906.

Tregear, R. T., and J. M. Squire. 1973. Myosin content and filament structure in smooth and striated muscle. *J. Mol. Biol.* 77:279–290.

Vainshtein, B. K. 1966. Diffraction of X-rays by Chain Molecules. Elsevier Publishing Co., Amsterdam, London and New York. 203–254.

Vibert, P. J., and R. W. Craig. 1982. Three-dimensional reconstruction of thin filaments decorated with a Ca^{2+}-regulated myosin. *J. Mol. Biol.* 157:299–319.

Winkelmann, D. A., H. Mekeel, and I. Rayment. 1985. Packing analysis of crystalline myosin subfragment-1. Implications for the size and shape of the myosin head. *J. Mol. Biol.* 181:487–501.